Asian Journal of Advanced Research and Reports

Volume 18, Issue 12, Page 426-435, 2024; Article no.AJARR.128248
ISSN: 2582-3248

Synthesis and Characterization of Magnetic Graphene-Oxide

Versha Rani [a*]

[a] *Department of Physics, Sri Ram Singh Dhoni Govt. Degree College, Jainti, 263626, Uttarakhand, India.*

Author's contribution

The sole author designed, analysed, interpreted and prepared the manuscript.

Article Information

DOI: https://doi.org/10.9734/ajarr/2024/v18i12840

Open Peer Review History:
This journal follows the Advanced Open Peer Review policy. Identity of the Reviewers, Editor(s) and additional Reviewers, peer review comments, different versions of the manuscript, comments of the editors, etc are available here: https://www.sdiarticle5.com/review-history/128248

Original Research Article

Received: 13/10/2024
Accepted: 15/12/2024
Published: 20/12/2024

ABSTRACT

Magnetic graphene-oxide has recently taken in research spotlight due to its extraordinary physical and chemical properties. Here, we report the synthesis of Graphene oxide based magnetic nano-composites with the size of (~13-14 nm) using simple chemical co-precipitation method. The composites were characterized by X-ray diffraction (XRD), Fourier transform infrared spectroscopy (FTIR) and vibrating sample measurement (VSM). It was observed that all the composites are superparamagnetic in nature. The saturation magnetization was observed to increase with the increasing magnetite nanoparticles (MNPs) in the composites. The dielectric properties of the composites were also improved by adding MNPs. These results remark that synthesized nanocomposites have great potential for magnetic, capacitive, microwave absorption and bio medical applications such as drug delivery, tumor treatment etc.

Keywords: Graphen-oxide; magnetic graphene-oxide; hysteresis; dielectric loss.

**Corresponding author: Email: vershachauhan31@gmail.com;*

Cite as: *Rani, Versha. 2024. "Synthesis and Characterization of Magnetic Graphene-Oxide". Asian Journal of Advanced Research and Reports 18 (12):426-35. https://doi.org/10.9734/ajarr/2024/v18i12840.*

1. INTRODUCTION

The graphene is a single or multi-layer 2D hexagonal honeycomb lattice sheet. These sheets are sp^2 hybridized and are separated about 1.4 Å from each other thus increasing the sheet strength (Tanwar & Mathur, 2020). Due to two-dimensional nature along with associated band structure, graphene and its composites are utilized in various applications such as supercapacitors, electronics, biosensing and photocatalysis (Bisht et al., 2017; Vestince et al., 2021; Vestince et al., 2021). Graphene and its derivative form graphene oxide are obtained from graphite (Rani et al., 2023). GO consists the polar surfaces with then attached functional groups C=O,C-O and –OH. Due to this polar surfaces, a number of materials like bio-molecules, metals, fluorescent moieties, drug molecules and nanoparticles can be easily attached with GO (Tanwar & Mathur, 2020).

Due to their unique chemical, physical, thermal and mechanical properties, magnetite nanoparticles (MNPs) offer a high potential for several applications in the field of environmental remediation, water purification, magnetic recording media, data storage, ferro-fluids as well as in various biomedical applications etc (Joshi et al. 2020; Mudila et al., 2020; Joshi et al., 2023). On other hand, MNPs has the large surface to volume ratio and therefore posses high surface energies. Then, they tend to aggregate so as to minimize the surface energies for being stable. Moreover, the MNPs have high chemical activity and easily oxidized in air resulting loss in magnetism. This comprise coating and grafting with organic molecules or surfactants, polymers, inorganic layers such as silica, metal, nonmetal etc (Mahdav et al., 2013).

Nano-composites of MNPs with GO have drawn a lot of attention due to their extensive applications in various fields such as drug delivery (León Félix et al., 2019), water purification (Abro et al., 2021), batteries (Kulal & Badalamoole, 2020), environmental remediation (Ahmadpour et al., 2020), electro-magnetic shielding (Bisht & Zaidi, 2015), water purification (Costa et al., 2019), microwave absorption (Chandra et al., 2010), sensors (Yunjin et al., 2012) and bio-medical etc. In the present work, we have fabricated graphene oxide doped magnetite nanocomposites (GOMNCs)with different weight ratios using chemical co-precipitation method. The structural, thermal, electrical and magnetic properties of prepared nanostructures were compared with that of GO and GOMNCs.

2. METHODOLOGY

2.1 Materials

Grapheme oxide, $FeCl_2 \cdot 4H_2O$, anhydrous $FeCl_3$, ammonia solution, hydrogen peroxide solution, sulfuric acid, hydrochloric acid and de-ionized water were used for the preparation of composites.

2.2 Preparation of GO-Fe_3O_4 Composites

GO was prepared according to literature reports via modified Hummer's method (Zaabaa et al., 2017). GOMNCs were prepared through chemical co-precipitation of $Fe_3O_4$from a composition of $FeCl_2.4H_2O$ and$FeCl_3.6H_2O$in 1:2 molar ratio supplemented with varying weight fractions of GO. The weight fractions of Fe (III) to GO was adjusted into 5:1, 8:1, 15:1 to afford the three samples of GOMNCs. For the preparation of GOMNCs involving Fe (III): GO(I), a suspension of GO (0.1g/dL, 50 mL) in deionized water was subjected to ultrasonic treatment over 45 min with simultaneous feeding of 50 mLa formulation of Fe (III):Fe (II) in 1:0.6 (w/w,50 mL) in deionized water @ 0.1 mL/min at 300K. Chemical co-precipitation of Fe_3O_4 in presence of GO was conducted through addition of ammonia solution (30%,v/v) at 85^0Ctill rise in pH level of reaction medium to 10.The contents were allowed for stirring @500 rpm over 180 min thereafter cooled to 300K and subsequently centrifuged at ~4000 rpm for 15 min. GOMNCs settled at the bottom of centrifuge tube were successively washed with deionized water till removal of chloride ions. GOMNCs were isolated from centrifuge tube through magnetic separation and dried at 400 mmHg/300K. Magnetite nanoparticles were also prepared following identical co precipitation method and served as reference for measurement of spectral and electrical, thermal and magnetic properties of GOMNCs.

2.3 Characterization

The microstructure and surface morphology of synthesized composites are observed using Scanning Electron Microscopy technique. The gain knowledge on phase transformation, the samples were analyzed with the XRD study. XRD analysis has been performed under Cu Ka radiation with a wavelength of 1.54059 A˚. Average crystallite size (D) of samples was

calculated using Scherrer's formula $D=0.93\lambda/\beta\cos\theta$, where λ is is the X-ray wavelength, β is the full width at half maximum in radian and θ is the angle of diffraction. Fourier transform infrared (FT-IR) spectroscopy was performed over the spectral range of 4000–500 cm^{-1} (Perkin Elmer Spectrum Two Version 10.03.06 with KBr pellets) to determine their crystal structure, bonding behavior and functional groups. The magnetic properties were being studied using Vibrating Sample Magnetometer (VSM). The room temperature (300K) magnetic properties of synthesized samples were studied using vibrating sample magnetometer (Quantum design PPMs, temp-range upto 2K, magnetic field-9 tesla). Dielectric measurements were performed for the frequency range 100 Hz and 1MHz using Automatic Hioki 3532-50 Hi teater LCR meter.

3. RESULTS AND DISCUSSION

3.1 Microstructure

The surface morphology of the GOMNCs were found out by using scanning electron microscopy. SEM images Fig. 1 show that GOMNCs were spherical in shape with a narrow particle size (~13-14 nm which is calculated by the Debye–Scherrer formula). Particles agglomeration is indicating a good connectivity between the grains all together. It looks like a smoothed sponge-like structure.

The X-ray diffraction pattern of natural graphite powder, GO and GOMNCs were shown in Fig. 2. Graphite shows a lattice planes of (002), (101) and (004) at $2\theta = 26.8^0$, 44.8^0 54.8^0 respectively with 0.33 nm spacing between the layers 5. (Rani et al., 2023). In the XRD pattern GO, peak (002) is shifted to 11.94, indicating that the interlayer spacing increases to 0.74 nm after oxidization 18. (Zaabaa et al., 2017; Alam et al., 2017). Due to the existence of oxygen functional groups, the interplanar spacing of GO is increased. XRD reveals the formation of MNPs with crystallite size ~17.5 nm bearing single-phase cubic spinel and lattice parameter $8.36A^0$ (Rahman et al., 2012). Addition of magnetite nano particles into GO rendered a series of diffraction peaks at angles 2θ (plane) = 30.30^0(220), 35.66^0(311), 43.35^0(400), 57.3^0(511), 63.0^0(440). Except the diffraction peaks assigned to magnetite nanoparticles, no other characteristic peaks result from GO can be observed in the XRD pattern of the composites system. It demonstrates the complete reduction of the GO. Moreover, there is no outstanding diffraction peak at ~26° as the result of uniform dispersion of GO on the surface of magnetite NPs, indicating exfoliation and preventing

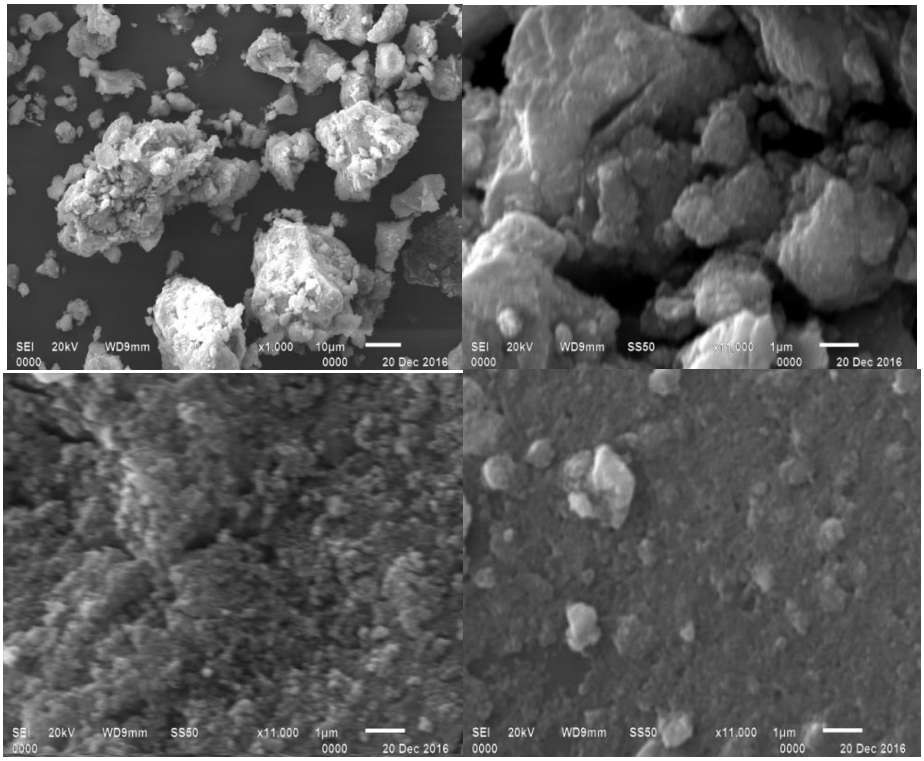

Fig. 1. SEM images of GO-Fe_3O_4 nano-composites at different magnifications

another restacking of the graphene sheets to larger extent (Shahid et al., 2015). The addition of GO has induced a surprising reduction in the crystallite size of magnetite NPs ranging 17.50 to 13-14 nm with retained cubic structure.

3.2 FTIR Study

The FTIR spectra of GO and GOMNCs are shown in Fig. 3. Upon oxidation of graphite to GO, the observed representative peaks of GO confirm the presence of the oxygen-containing functional moieties in carbon frameworks, which include the bands at ~1040 cm^{-1} (C-O stretching vibration of epoxide), 1420 cm^{-1} (tertiary C-OH groups stretching), and 1720 cm^{-1} (C=O stretching of carbonyl and carboxyl groups located at edges of the GO networks). Moreover, signature of aromatic C=C stretching at ~1576 cm^{-1} indicates the presence of sp^2 hybridized honeycomb lattice (Manoratne et al., 2017). Peak around at 3414 cm^{-1} shows that moisture content in GO. The small signals located at 1965 cm^{-1} may belong to aromatic ring. These bands confirm the formation of GO from the oxidation of graphite powder.

In the FTIR spectrum, there are normally four sets of lattice vibrations, corresponding to lower and higher frequencies. The lattice vibrations involving oxygen and cations at octahedral and tetrahedral positions in the base lattice appear in the high frequency region, namely, v_1 and v_2 at 600–540 cm^{-1} and 400–460 cm^{-1}, respectively. The low frequency bands in the vicinity of 320 cm^{-1} are due to divalent oxygen vibrations. The typical M–O bond corresponds to a major banding the range of 550 to 553 cm^{-1} (tetrahedral) and a faint peak at430 cm^{-1} (octahedral lattice vibrations). The peak at 1387 $cm^{-1}$is due to the asymmetrical stretching vibrations of adsorbed carbonate ions CO_3^{2-} on the lattice.

In the FTIR spectrum of GOMNCs, band ranging 445 cm^{-1}-625 cm^{-1} attributed to vibrational modes of Fe-O confirms the occupancy of ferric ion (Fe^{+3}) at tetrahedral sites. The band at about 453 cm^{-1} corresponds to the presence of Fe-O bond at octahedral sites in the composites due to the magnetite phase (Rani et al., 2017; Rani et al., 2023).

3.3 Thermal Studies

The TG thermogram of GO also reveals the two step decomposition behavior (Fig. 4 (a)). The first weight loss 8.27% of GO occurs in the temperature range of 30^0 C -105^0C. The decomposition of GO starts at TG onset 161^0C with the weight loss 14.6%. The first step decomposition occurs in the temperature range of 161^0C -233^0C. 14.6% weight loss was found in this temperature range. Within this range of temperature, the oxygen bearing functionalities presenting over the graphitic surface of GO has been removed, converting this into graphite. On further heating of GO from 233°C to 441°C with weight loss of 10.9%, a steep loss has been recorded, due to the oxygen containing groups.CO_2 (2350 cm^{-1} and 690 cm^{-1}) and H2O (1340-1900 cm^{-1} and 3550-4000 cm^{-1}) are the products of this decomposition as expected in the FTIR spectra of GO (Fig. 3). Beyond this temperature, the thermal degradation of GO waspropose with rapid weight loss 49% till TG endset 566^0C for the second step decomposition. The decomposition of GO was at 1000°C leaving the residue13.74 due to formation of carbon black.

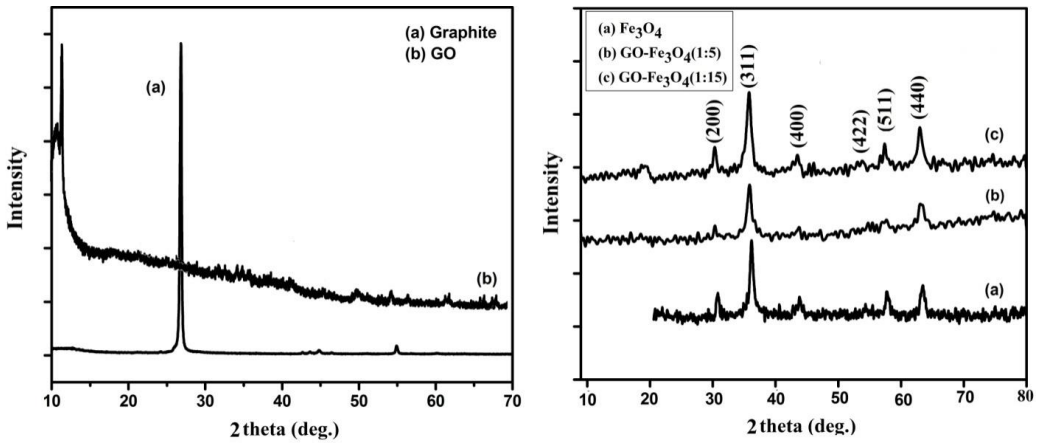

Fig. 2. XRD of Graphite, Graphene Oxide and GO-Fe_3O_4 nanocomposites

GOMNCs (I) starts decomposition at TG onset of 100^0 C with the weight loss 3.8% (Fig. 4 (a)). It may be due to the presence of water molecules in the nanocomposites. Afterwards, the 6.2% weight loss occurs in the temperature range of 100^0C-359^0C. Beyond this temperature, it occurs in the temperature range of 100^0C-359^0C. Beyond this temperature, it is decomposed with a rapid weight loss of 7.7% till TG end set temperature 472^0C. On further heating, there is no weight loss. For GOMNCs (III), only 3.02% weight loss was observed up to 100^0C (Fig. 4 (a)). Beyond this temperature, 4.24% weight loss occurs till the 300^0 C. On further heating, it was degraded with the weight loss 6.74% till the end set temperature 471^0C. Thus, a remarkable increase in thermal stabilty of GOMNCs (III) was observed over GOMNCs (I). Decomposition of GO was terminated in the temperature range 441-566^0C leaving char residue of (%, w/w) 14.4, whereas GOMNCs (I) and GOMNCs (III) leaves char residue of 82.5 and 86 at 472^0C and 471^0C, respectively.

In order to have the comparative study of thermal stability of the GO based composites , their repective TG data were compared at 300^0C and 600^0C (Fig. 4. (a)). At the 300^0C weight residue (%) GO, Magnetite, GOMNCs (I) and GOMNCs (III) are 68,97.8, 91. and 92.74. This remarks the higher thermal stability of magnetite over GO and overall thermal stabilty of the GOMNCs. At 600^0C weight losses (%) associated with GO, Magnetite, GOMNCs (I) and GOMNCs (III) 85, 2.04, 17.5 and 14.04 respectively. Such weight losses associated higher thermal stabilty of GO-Fe_3O_4 (III) over GO-Fe_3O_4 (I). On further heating, no weight loss was observed for GO and GOMNCs. Thus, synthesized nanocomposites diplay higer stabilty over GO.

GOMNCs (I) revealed the heat of decomposition of -1.17 J/mg 417^0 C with the DTA signal 4.8 μV respectively (Fig. 4. (b), (c)).GOMNCs(III)shows two DTA peaks at 428 ^{0}C and 516 ^{0}C with 42.2 μV and 10.7 μV acommpanied by heat of composition -922 mJ/mg and -44.5 mJ/mg respectively. Such increase in heat of decomposition DTA peak temperature also further accounted for the increase in the thermal stabilty of the graphene based nano composites with the proportinal to magnetite nanoparticles. DTG revealed the rate of decomposition (μg/min) for GOMNCs(I)is 67 and 110 corresponding peak temperatures (^{0}C) 63 and 429.

3.4 Magnetic Properties

Fig. 5 shows the magnetic field dependence of magnetization (M-H) curves of MNPs and GOMNCs. The magnetization was recorded at 300K with the maximum field of 40K Oe. The samples exhibit immeasurable values of coercive field and remnant magnetization which shows the superparamagnetic nature of all samples. The saturation magnetization of the GOMNCs (I) and GOMNCs (III) [~38 emu/g and ~46 emu/g respectively] is smaller than the value of bulk MNPs [~70.5emu/g] (Liang & Lu, 2020). It is observed that saturation magnetization value in GOMNCs decreases by adding GO into the MNPs (Table 1.). This can be attributed to the small particle size and relatively low amount of MNPsin the GOMNCs.

3.5 Dielectric Properties

Dielectric permittivity (ε') and los tangent (tan δ) of the GOMNCs as the function of frequency at the room temperature are shown in Fig. 6. The dielectric permittivity, which is also known as the relative dielectric constant, is the real part of the complex dielectric permittivity (ε = ε'- jε"). The Loss tangent (tan δ=ε"/ε') is commonly used as a measure of the energy dissipation in the dielectric materials. From Fig. 6 remarked the dielectric permittivity for GOMNCs get enhanced with the MNPs. It could also be noted that the dielectric loss (Fig. 6 (b)) of these composite system shows the little improvements with the addition of MNPs. This may be due to the rotation of Fe^{3+}-Fe^{2+} diploes. It may be viewed as the interchange of electrons between the ions so that the dipoles align themselves with the field. Thus the higher value of dielectric constant at low frequency is mainly due to the space charge polarization and rotation direction polarization. The contribution of rotation direction polarization becomes less at higher frequency because the dipole now cannot follow the quickly changing electric field so we obtained a decreasing pattern of ε' with increasing frequency.

The dielectric loss is found to be decreased with the addition of MNPs into the composite system. This reveals that the high dielectric loss observed in the GOMNCs. It may also be due to the electronic conductivity of GO. With the addition of MNPs leads the reduction of electronic conductivity of the composites. The variation of ε' and dielectric loss with frequency is similar to the behavior of grphene-oxide/Zn$_x$Fe$_{1-x}$Fe$_2$O$_4$. It can be evident from this study that dielectric properties can be tuned according to MNPs.

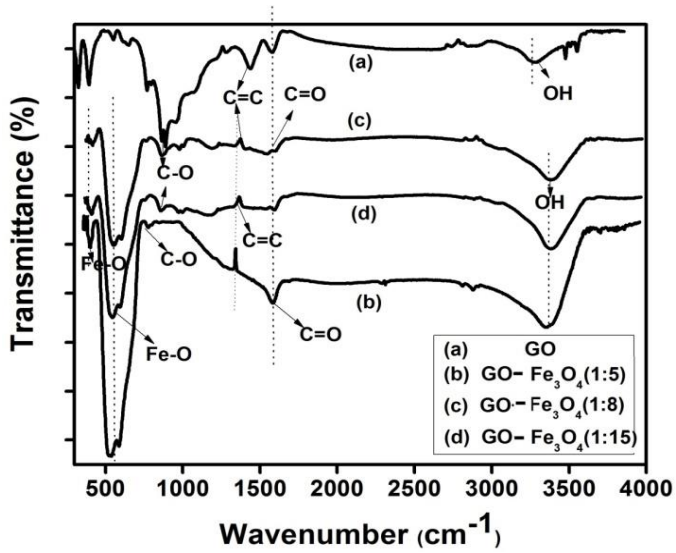

Fig. 3. FTIR Spectra of GO and GO-Fe_3O_4 nanocomposites

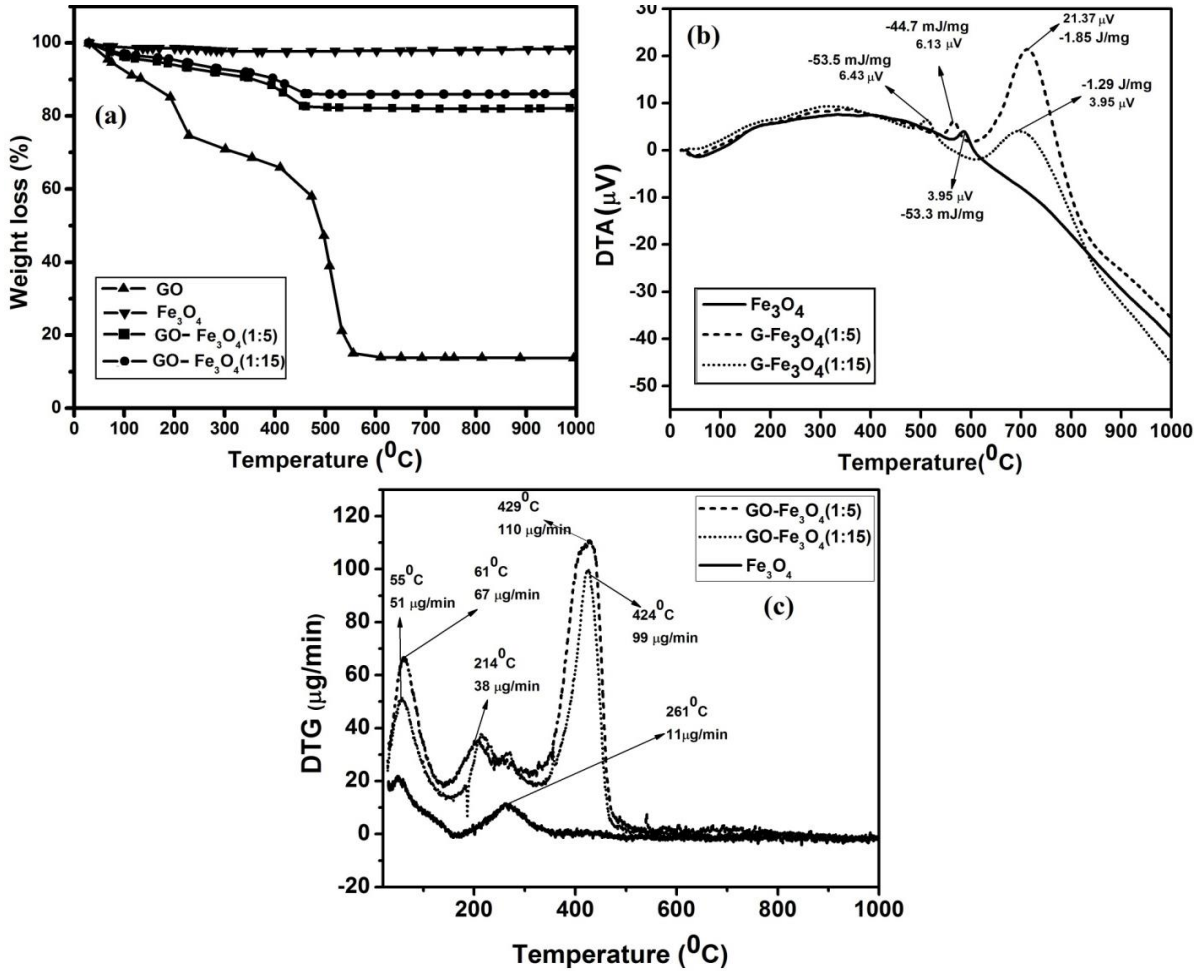

Fig. 4. TGA, DTA and DTG graph of GO and GO-Fe_3O_4 nanocomposites

Table 1. Magnetic properties Fe_3O_4 NPs and GO-Fe_3O_4 nanocomposites

Samples	Saturation magnetization (emu/gm)	Standard error	Coercivity (Oe)	Remnant magnetization (emu/gm)	M_r/M_S
Fe_3O_4 NPs	70.403	0.158	25.384	3.469	0.0493
GOMNCs **(I)**	37.868	0.057	14.051	1.294	0.0342
GOMNCs **(III)**	46.560	0.083	19.042	1.748	0.0375

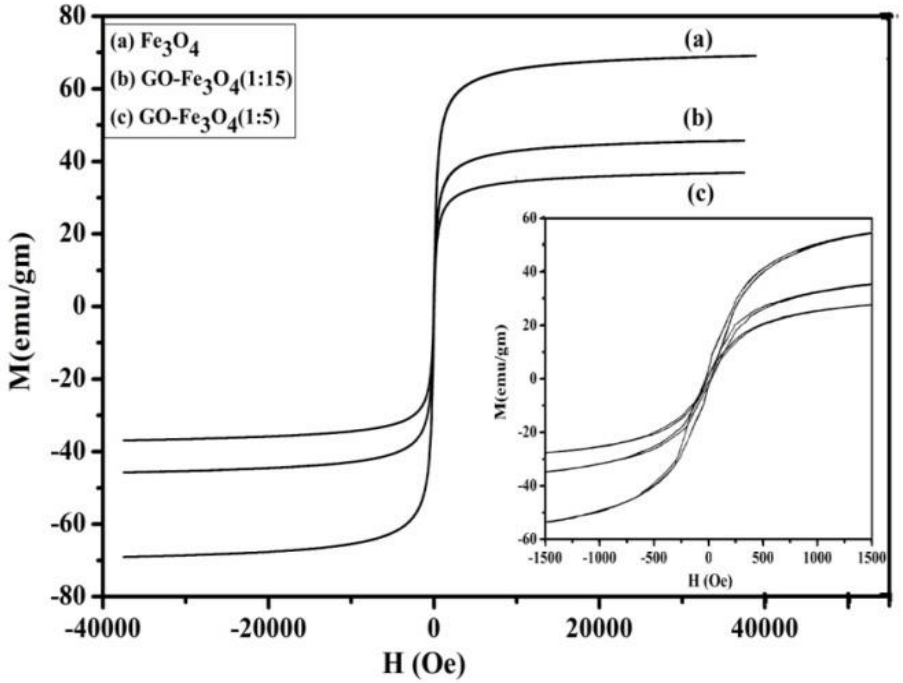

Fig. 5. VSM of Fe_3O_4 NPs and GO-Fe_3O_4 nanocomposites

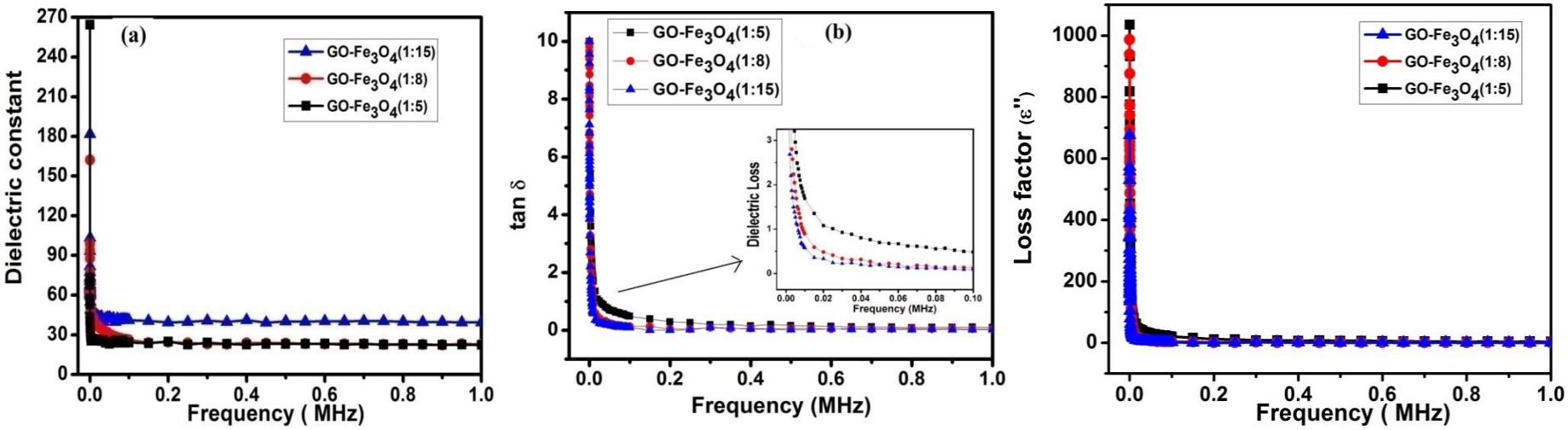

Fig. 6. Dielectric Constant and (b) Dielectric loss variation with Frequency (307 K) for GO-Fe_3O_4 nanocomposites

4. CONCLUSION

This study is investigated the synthesis of super paramagnetic graphene oxide with magnetite nano particles using simple the co-precipitation method. Surface morphology, X-ray diffraction and flourier transform infrared spectra displayed the magnetite nanoparticles are successfully attached with the graphene oxide. Synhesized nano system the different magnetic and dielectric properties with their pristine form. The graphene oxide based magnetite nano composites with superparamagnetic behavior provide the opportunities for various applications in the fields of biomedicine, drug delivery, tumor treatment, bio-material separation and bio-diagnostics, etc.

DISCLAIMER (ARTIFICIAL INTELLIGENCE)

Author(s) hereby declare that NO generative AI technologies such as Large Language Models (ChatGPT, COPILOT, etc) and text-to-image generators have been used during writing or editing of this manuscript.

ACKNOWLEDGEMENTS

Authors would like to acknowledge the Instrumentation Centre (IIT Roorkee) for providing the instrumentation facilities.

COMPETING INTERESTS

Author has declared that no competing interests exist.

REFERENCES

Abro, K. A., Khan, I., & Gomez-Aguilar, J. F. (2021). Thermal analysis in nanotechnology. *Journal of Thermal Analysis and Calorimetry*, *143*(5), 3633.

Ahmadpour, N., Sayadi, M. H., Sobhani, S., & Hajiani, M. (2020). Environmental management practices. *Journal of Environmental Management*, *271*, 110964.

Alam, S. N., Sharma, N., & Kumar, L. (2017). Graphene materials for advanced applications. *Graphene*, *6*(1), 1–7.

Bisht, G., & Zaidi, M. G. H. (2015). Drug delivery innovations. *Drug Delivery and Translational Research*, *5*, 268.

Bisht, G., Zaidi, M. G. H., & Rayamajhi, S. (2017). Advanced polymeric materials and biomaterials. *International Journal of Polymeric Materials and Polymeric Biomaterials*, *66*(14), 708.

Chandra, V., Park, J., Chun, Y., Lee, J. W., Hwang, I. C., & Kim, K. S. (2010). Graphene-based nanomaterials. *ACS Nano*, *4*, 3979.

Costa, A. C. S., Alves, H. P. A., Correa, M. A., Bohn, F., & Acchar, W. (2019). Material development in physical chemistry. *Materials Chemistry and Physics*, *232*, 1.

Joshi, I., Rani, V., Joshi, P., & Khati, K. (2023). Green chemistry for material science. *Bulgarian Chemical Communications*, *55*(A), 1–7.

Joshi, S. K., Kumar, A., & Zaidi, M. G. H. (2020). Development of nanomaterials in defense applications. *Defence Science Journal*, *70*(3), 306.

Kulal, P., & Badalamoole, V. (2020). Natural biopolymers for medical use. *International Journal of Biological Macromolecules*, *165*, 542.

León Félix, L., Sanz, B., Sebastián, V., Torres, T. E., Sousa, M. H., Coaquira, J. A. H., Ibarra, M. R., & Goya, G. F. (2019). Magnetic nanoparticle research. *Scientific Reports*, *9*, 4185.

Liang, Y., & Lu, W. (2020). Electronic materials for advanced technologies. *Journal of Materials Science: Materials in Electronics*, *31*(19), 17075–17083.

Mahdav, M., Ahmad, M. B., Haron, M. J., Namvar, F., Nadi, B., Zaki, M., Rahman, A., & Amin, J. (2013). Nanostructured materials for biomedical applications. *Molecules*, *18*(7), 7533–7548.

Manoratne, C. H., Rosa, S. R. D., & Kottegoda, I. R. M. (2017). Applications of material science. *Materials Science Research India*, *14*(1), 19–30.

Mudila, H., Parashr, P., Kapoor, H. L., Rana, S., & Zaidi, M. G. H. (2020). Electrochemical studies in material development. *Portugaliae Electrochimica Acta*, *38*(2), 69.

Rahman, O. U., Mohapatra, S. C., & Ahmad, S. (2012). Synthesis and properties of materials. *Materials Chemistry and Physics*, *132*, 196–202.

Rani, V., Joshi, I., Rawat, P. S., & Srivastava, R. C. (2023). Green approaches in chemical engineering. *Bulgarian Chemical Communications*, *55*(A), 1–6.

Rani, V., Joshi, I., Rawat, P. S., & Srivastava, R. C. (2023). Natural bioresources for chemical applications. *Bulgarian Chemical Communications*, *55*(A), 1–5.

Rani, V., Srivastava, R. C., Agarwal, H. M., & Zaidi, M. G. H. (2017). Nanostructure developments. *Materials Today: Proceedings*, *4*(9), 9471.

Shahid, A., Iftikhar, G. H., Nasir, M., & Muhammad, M. (2015). Characterization of advanced materials. *Materials Characterization*, *99*, 254–265.

Tanwar, S., & Mathur, D. (2020). A review on materials synthesis. *Materials Today: Proceedings*, *30*(1), 17–22.

Urade, A. R., Lahiri, I., & Suresh, K. S. (2022). Recent advancements in material science. *Springer Nature*, *75*(3), 614–630.

Vestince, B., Mbayachi, N., Ndayiragije, E., Sammani, T., Taj, S., Mbuta, E. R., & Khan, A. U. (2021). Antimicrobial applications of green chemistry. *Results in Chemistry*, *3*, 100163.

Yunjin, Y., Shiding, M., Shizhen, L., Li Ping, M., Hongqi, S., & Shaobin, W. (2012). Chemical engineering for environmental sustainability. *Chemical Engineering Journal*, *184*, 326.

Zaabaa, N. I., Fooa, K. L., Hashima, U., Tan, S. J., Liu, W. W., & Voon, C. H. (2017). Advances in engineering materials. *Procedia Engineering*, *184*, 469–477.

Peer-review history:
The peer review history for this paper can be accessed here:
https://www.sdiarticle5.com/review-history/128248